The Astrophysical Journal Letters, 907:L38 (6pp), 2021 February 1 https://doi.org/10.3847/2041-8213/abd698

Water Production Rate of C/2020 F3 (NEOWISE) from SOHO/SWAN over Its Active Apparition

M. R. Combi[1], T. Mäkinen[2], J.-L. Bertaux[3], E. Quémerais[3], and S. Ferron[4]
[1] Department of Climate and Space Sciences and Engineering, University of Michigan, 2455 Hayward Street, Ann Arbor, MI 48109-2143, USA; mcombi@umich.edu
[2] Finnish Meteorological Institute, Box 503, SF-00101 Helsinki, Finland
[3] LATMOS/IPSL Université de Versailles Saint-Quentin 11, Boulevard d'Alembert, 78280, Guyancourt, France
[4] ACRI-st, Sophia-Antipolis, France
Received 2020 December 2; revised 2020 December 22; accepted 2020 December 23; published 2021 January 29

Abstract

C/2020 F3 (NEOWISE) was discovered in images from the Near Earth Object program of the Wide-Field Infrared Survey Explorer (NEOWISE) taken on 2020 March 27 and has become the Great Comet of 2020. The Solar Wind ANisotropies (SWAN) camera on the Solar and Heliospheric Observatory (SOHO) spacecraft, located in a halo orbit around the Earth–Sun L1 Lagrange point, makes daily full-sky images of hydrogen Lyα. Water production rates were determined from the SWAN hydrogen Lyα brightness and spatial distribution of the comet measured over a 4 month period of time on either side of the comet's perihelion on 2020 July 3. The water production rate in s^{-1} was moderately asymmetric around perihelion and varied with the heliocentric distance, r, in au as $(6.9 \pm 0.5) \times 10^{28}\ r^{-2.5\pm0.2}$ and $(10.1 \pm 0.5) \times 10^{28}\ r^{-3.5\pm0.1}$ before and after perihelion, respectively. This is consistent with the comet having been through the planetary region of the solar system on one or more previous apparitions. Water production rates as large as $5.27 \times 10^{30}\ s^{-1}$ were determined shortly after perihelion, once the comet was outside the solar avoidance area of SWAN, when the comet was 0.324 au from the Sun.

Unified Astronomy Thesaurus concepts: Comets (280); Comae (271); Neutral coma gases (2158); Long period comets (933); Comet origins (2203); Oort cloud (1157)

1. Introduction

Comet C/2020 F3 (NEOWISE), hereafter comet NEOWISE, is an Old Long-period comet, using the A'Hearn et al. (1995) classification, discovered in images taken on 2020 March 27 by the Near Earth Object program of the Wide-Field Infrared Survey Explorer (NEOWISE). Its orbit had an inbound semimajor axis of 270 au and is projected to have an outbound semimajor axis of 255 au. It reached perihelion on July 3 at a distance of 0.295 au from the Sun. It became a spectacular visual naked-eye object for a few weeks near perihelion. Its semimajor axis indicates that it is definitely not a dynamically new comet directly from the Oort cloud and so has been through the planet region of the solar system on previous apparitions.

The Solar Wind ANisotropies (SWAN) camera on the Solar and Heliospheric Observatory (SOHO) spacecraft observed the Lyα emission from atomic hydrogen throughout its apparition. SWAN makes all-sky observations of the Lyα emission of interstellar atomic hydrogen that streams through the solar system and is removed by solar radiation and solar charged particle impact leaving a characteristic distribution that is bright in the direction of incoming hydrogen atoms and fainter in the downstream direction of outgoing hydrogen atoms (Bertaux et al. 1995). The typical interplanetary hydrogen Lyα brightness ranges from about 0.5 kilorayleighs up to several kilorayleighs in directions near the Sun.

SWAN's 5 by 5 one-degree detectors scan across the sky daily, making a full-sky image, excluding an avoidance region around the Sun and another region blocked by parts of the spacecraft itself. SOHO has been located in a halo orbit around the L1 Earth–Sun Lagrange point since a few months after its launch in 1995 December. Most instruments are still operating nominally, including SWAN. A comet is detectable when its hydrogen Lyα brightness is larger than about 100 Rayleighs so it is distinguishable by its spatial distribution above that of the interplanetary signal. This typically happens for comets that are brighter than between magnitude 12–10 in the visible. Cometary signals as bright as 20–30 kilorayleighs, which do not saturate the detectors, can be reliably detected. Observations at the faint end are typically limited by the interplanetary brightness, especially near the Sun, and by the occurrence of nearby bright stars, especially when a comet is near the galactic equator.

2. Model Analysis

Observations of a comet's hydrogen coma are analyzed in order to calculate the water production rate of the comet, relying on the fact that water is typically the most abundant volatile gas in the coma when comets are within about 3 au from the Sun (Combi et al. 2005; Mäkinen & Combi 2005). Water is photodissociated into a well-known distribution of possible fragment H and O atoms, H_2 molecules, OH radicals, and their ions (Combi et al. 2004). Since SOHO's launch in 1995 water production rates have been determined from SWAN observations of over 70 comets (Bertaux et al. 1998; Combi et al. 2019; Combi 2020a).

Comet NEOWISE was detectable and first distinguishable from background stars in SWAN images beginning on 2020 May 12. It was detected from then until June 19 when it entered the solar avoidance area. Enough of the coma to be useful for analysis was clearly detectable beginning on July 6 and remained detectable until September 2.

Figure 1 shows an image of the H Lya coma observed by SWAN on 2020 July 9 when it was near its maximum. Since the solar fluorescence rate of hydrogen Lyα is rather large, radiation pressure on the hydrogen atoms produces what is essentially a

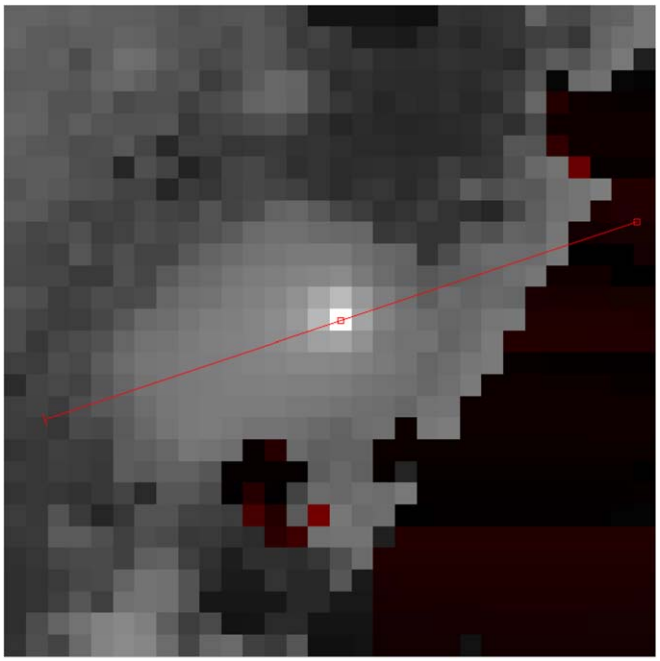

Figure 1. SOHO/SWAN image of the hydrogen coma of comet C/2020 F3 (NEOWISE) observed on 2020 July 9. The field of view is 30° across. The straight line from left to right and slightly upward shows a profile cut along the maximum extent of the hydrogen "tail" whose profile is shown in Figure 2. The dark region toward the right and lower right corresponds to the solar avoidance area of SWAN with the direction to the right to the Sun.

broad hydrogen "tail" pointed away and lagging behind the direction of the comet in its orbit around the Sun. The extent of the asymmetry and of the general shape of the hydrogen coma is determined by velocity distributions of H atoms leaving the inner partially collisional coma (Combi & Smyth 1988; Combi et al. 2000). While H atoms are produced at a dominant velocity of $\sim$18 km s^{-1} upon photodissociation of water and $\sim$8 km s^{-1} upon photodissociation of OH, when coma production rates are large, and especially for a smaller heliocentric distance when photochemical lifetimes are smaller, collisions of the fast nascent hydrogen atoms with the slow outflowing heavy molecules partially thermalize and slow part of the distribution of hydrogen atoms. For a large production rate comet like C/2020 F3 (NEOWISE) at small heliocentric distances (0.3–0.5 au) a significant fraction of the hydrogen atoms are slowed to velocities from 8–18 km s^{-1} to 1–4 km s^{-1}, elongating and narrowing the antisunward distribution of the hydrogen tail. Figure 2 shows the profile cut through the hydrogen coma indicated by the straight line in Figure 1. In the model that we use, the nascent velocity distribution is determined solely by the known photodissociation branches of water and OH, and the velocity distribution of the atoms exiting the inner partially collisional coma is determined by the level of the water production rate. The velocity distribution then is not a fitting parameter, but a consequence of the level of the production rate and the heliocentric distance. Therefore, the fact that the model reproduces the spatial distribution of the coma is a demonstration that the fixed parameterization of the coma physics is correct given the linear relationship between the observed brightness and abundance as well as the nonlinear relationship between the spatial distribution of the brightness and the photochemical and collisional physics in the model.

Water production rates were calculated from all hydrogen coma images using the method described in detail by Mäkinen & Combi (2005). Water production rates were calculated from each SWAN image of comet F3 (NEOWISE) for 74 days beginning on 2020 May 13 and running through 2020 September 2. There was a large data gap from June 18 until July 7 when the comet was too close to the Sun in the sky for SWAN to obtain images of the region of the sky where the comet was located. The first post-perihelion production rate obtained when the comet was on 0.324 au from the Sun on July 7 was 5.15×10^{30} s^{-1}, one of the largest water production rates obtained by SWAN since comet C/1995 O1 (Hale–Bopp; Combi et al. 2000). For Hale–Bopp Combi et al. (2000) explained that for a brightness less than $\sim$30 kilorayleighs optical depth effects in the SWAN aperture could be neglected. For F3 (NEOWISE) the brightest pixel centered on the nucleus has a comparable brightness, but this is only because the smallest heliocentric distance is $\sim$0.33 au when the comet was nearly this bright and the illuminating flux from the Sun was $\sim$8 times larger than it was for Hale–Bopp at perihelion and column densities similarly many times lower. Therefore, optical depth effects for F3 (NEOWISE) are much less of an issue.

Table 1 gives the observational circumstances, g-factors, the water production rates, and their formal 1σ uncertainties. Figure 3 shows the variation of the water production rate as a function of time in days measured from perihelion on 2020 July 3. The vertical lines through each point give the formal 1σ error bars that result from the fitting procedure to the hydrogen coma model and the interplanetary hydrogen Lyα sky background. Actual systematic uncertainties resulting from the model, model parameters, and the absolute calibration of SWAN, the LASP solar Lyα irradiances, and the solar Lyα line profile are estimated to be on the order of 30%. It appears that the water production rate at perihelion when SWAN could not observe it was on the order of nearly 10^{31} s^{-1}.

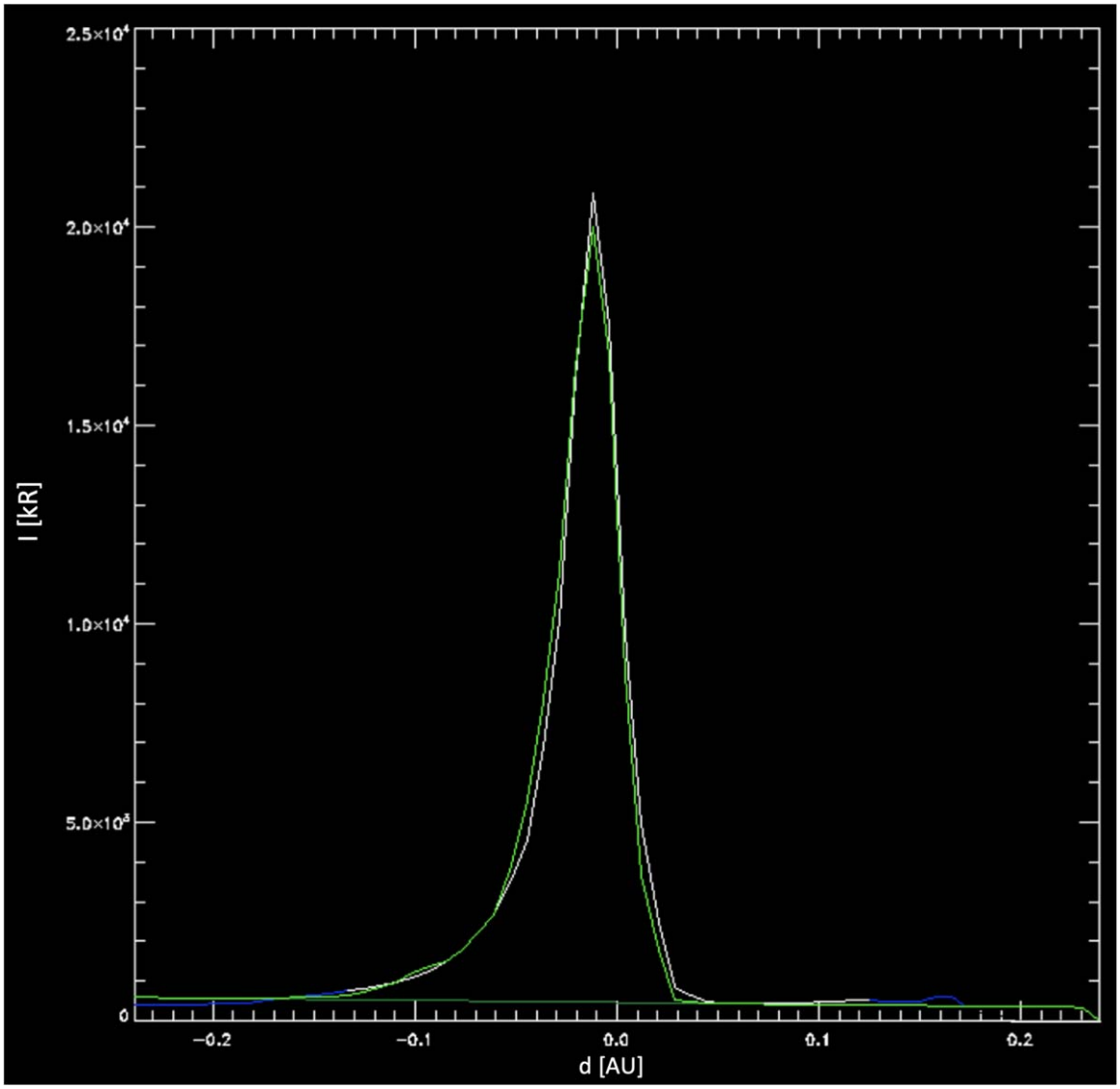

Figure 2. Model–data comparison profile along the long extent of the hydrogen "tail" of comet C/2020 F3 (NEOWISE) observed by SOHO/SWAN on 2020 July 9. The white curved line corresponds to the observed brightness along the cut shown in Figure 1 along the maximum extent of the hydrogen tail. The flat straight green line near the bottom corresponds to the fitted interstellar hydrogen background. The curved green line is the fit of the coma model to the observed image. The red line toward the lower right is where the observed profile cuts through a field star that has been marked to be ignored. Note that the shape of the model profile follows the asymmetric coma distribution that is produced by radiation pressure from the resonance scattering of the same solar Lyα photons that enable us to observe the hydrogen coma. The asymmetric shape itself is a property of the model parameterization itself and not a free fitting parameter. The fact that it reproduces the data indicates that the model works well even under these extreme conditions of high production rate and small heliocentric distance.

3. Discussion

It is often instructive to look at a power-law fit of the water production rate as a function of heliocentric distance both before and after perihelion. Figure 4 shows the water production rate plotted as a function of heliocentric distance with pre- and post-perihelion data plotted in separate panels. The straight lines are the best-fit power laws. In the survey of 61 comets observed by SOHO/SWAN, Combi et al. (2019) have shown there is a consistent pattern of variation of the average and range of pre- and post-perihelion power-law exponents as a function of the dynamical age of long-period comets, with the flattest slopes found in Dynamically New comets ($1/a_o < 50 \times 10^{-6}$) and gradually more steeper slopes in Young Long-period (50×10^{-6} $1/a_o < 2000 \times 10^{-6}$) and Old Long-period comets ($1/a_o > 2000 \times 10^{-6}$), using the A'Hearn et al. (1995) dynamical age classification. The power-law fits to the water production rates are $(6.9 \pm 0.5) \times 10^{28}$ $r^{-2.5\pm0.2}$ and $(10.1 \pm 0.5) \times 10^{28}$ $r^{-3.5\pm0.1}$ before and after perihelion, respectively, with the production rate in s^{-1} and the heliocentric distance, r, in au. The pre-perihelion power-law exponent determined for C/2020 F3 (NEOWISE) is near the middle of the range of comets, in the same dynamical Old Long-period classification from the survey. The post-perihelion exponent is also consistent, being in the same range with comets that are similarly Old Long-period in the survey. The deviations of the actual production rate determination from the power-law fits are surprisingly small, showing that there were no major outbursts or quiescent episodes.

Bauer et al. (2020) have estimated a nucleus diameter of ~5 km for this comet from WISE spacecraft observations by subtracting a fitted dust coma model. This means that the nucleus is only slightly larger than that of the Rosetta target comet 67P/Churyumov–Gerasimenko, which had a mean diameter of ~4 km. The water production rate of 67P was in

Table 1
SOHO/SWAN Observations of C/2020 F3 (NEOWISE) and Water Production Rates

ΔT[a]	r[b]	Δ[c]	g[d]	Q[e]	δQ[f]
(days)	(au)	(au)	(s^{-1})	(10^{28} s^{-1})	(10^{28} s^{-1})
−51.553	1.295	1.603	0.001786	6.17	0.35
−50.552	1.276	1.604	0.001815	2.72	0.87
−49.552	1.257	1.604	0.001780	4.31	0.51
−48.552	1.238	1.604	0.001780	6.01	0.40
−46.575	1.200	1.605	0.001815	5.00	0.31
−44.580	1.161	1.604	0.001798	5.56	0.50
−41.580	1.102	1.603	0.001830	5.49	0.46
−33.634	0.941	1.590	0.001875	6.81	0.45
−31.634	0.900	1.584	0.001889	6.98	0.47
−30.634	0.879	1.581	0.001913	5.78	0.51
−29.637	0.858	1.577	0.001892	7.24	0.47
−28.636	0.836	1.573	0.001890	8.54	0.38
−27.637	0.815	1.569	0.001915	8.59	0.56
−26.636	0.793	1.564	0.001908	12.25	0.28
−25.663	0.772	1.560	0.001938	11.40	0.29
−24.662	0.751	1.554	0.001948	11.92	0.30
−23.663	0.729	1.548	0.001962	12.10	0.31
−22.664	0.707	1.542	0.001955	17.12	0.23
−21.664	0.685	1.535	0.001953	23.21	0.19
−20.664	0.663	1.528	0.001955	19.83	0.22
−19.692	0.641	1.520	0.001957	20.14	0.77
−18.692	0.619	1.511	0.001959	30.76	1.96
−17.692	0.597	1.502	0.001928	22.70	3.34
−15.819	0.555	1.483	0.001924	33.48	0.15
−15.693	0.552	1.482	0.001923	42.06	0.13
−14.693	0.530	1.471	0.001869	50.46	0.15
4.203	0.324	1.011	0.001471	514.80	123.30
5.200	0.337	0.976	0.001520	527.30	0.07
6.174	0.352	0.944	0.001570	523.40	0.05
7.174	0.369	0.911	0.001620	364.20	0.05
8.172	0.387	0.880	0.001665	319.50	0.04
9.145	0.406	0.852	0.001707	220.50	0.05
10.145	0.426	0.824	0.001708	166.10	31.05
11.144	0.446	0.799	0.001753	220.80	0.03
12.116	0.467	0.777	0.001763	168.20	0.03
13.116	0.488	0.756	0.001752	160.40	0.03
13.412	0.495	0.751	0.001735	95.40	0.04
15.440	0.539	0.719	0.001757	109.80	0.03
25.043	0.752	0.727	0.001721	25.77	0.07
26.043	0.774	0.741	0.001744	23.41	0.08
27.043	0.795	0.757	0.001727	21.68	0.09
28.044	0.817	0.775	0.001720	21.66	0.08
29.064	0.839	0.795	0.001715	19.55	0.07
30.064	0.860	0.816	0.001727	14.88	0.10
31.064	0.881	0.839	0.001765	15.26	0.20
32.073	0.902	0.863	0.001757	13.36	0.52
33.073	0.923	0.888	0.001745	12.02	0.11
35.092	0.965	0.940	0.001765	9.27	0.72
36.092	0.985	0.968	0.001784	8.54	0.26
37.092	1.006	0.996	0.001777	7.52	0.16
38.102	1.026	1.025	0.001763	8.45	0.76
39.102	1.047	1.054	0.001760	6.17	0.69
40.102	1.067	1.083	0.001770	6.81	0.14
41.121	1.087	1.114	0.001739	6.56	0.18
42.121	1.107	1.144	0.001745	6.37	0.19
43.121	1.126	1.175	0.001732	4.47	0.30
44.121	1.146	1.206	0.001720	5.06	0.25
45.131	1.166	1.237	0.001721	5.87	0.26
46.131	1.185	1.268	0.001728	2.55	0.58
47.131	1.204	1.300	0.001688	5.56	0.30
48.131	1.224	1.331	0.001693	3.84	0.45
49.131	1.243	1.363	0.001686	1.62	1.03
50.147	1.262	1.395	0.001688	4.89	0.36
51.147	1.281	1.427	0.001694	6.63	0.25
52.147	1.300	1.459	0.001682	3.95	0.43
53.147	1.318	1.491	0.001675	4.98	0.40
54.148	1.337	1.523	0.001645	6.49	0.33
55.147	1.355	1.554	0.001661	3.44	0.57
56.157	1.374	1.587	0.001672	4.75	0.89
57.157	1.392	1.619	0.001660	5.90	0.40
58.157	1.411	1.650	0.001667	2.04	1.00
59.157	1.429	1.683	0.001655	1.41	1.23
60.157	1.447	1.714	0.001676	7.43	0.28
61.157	1.465	1.746	0.001669	3.55	0.50
62.157	1.483	1.778	0.001653	1.90	0.95
63.157	1.501	1.809	0.001646	5.05	0.50
64.174	1.519	1.841	0.001635	2.87	0.63
65.157	1.536	1.872	0.001651	3.38	0.64
66.174	1.554	1.903	0.001644	2.75	0.68

Notes. Notes to Table 1.
[a] Days from perihelion 2020 July 3.679.
[b] Heliocentric distance (au).
[c] SOHO/comet distance (au).
[d] Solar Lyα g-factor (photons s^{-1}) at 1 au.
[e] Water production rates for each image (10^{28} s^{-1}).
[f] Internal 1σ uncertainties (10^{28} s^{-1}).

the range of 1–3 × 10^{28} s^{-1} (Bertaux et al. 2014; Biver et al. 2019; Combi et al. 2020b) when it reached its perihelion of 1.24 au. When C/2020 F3 (NEOWISE) was at a heliocentric distance of 1.2–1.3 au its water production rate was in the range of 4–6 × 10^{28} s^{-1} (Table 1). Whereas the production rate of NEOWISE was a factor 2–4 times larger than that of 67P at the same heliocentric distance, its surface area is about 56% larger. So, while 67P had an active surface fraction in the range of 4%–8%, that of NEOWISE was on the order of 8%–20%.

4. Summary

Comet C/2020 F3 (NEOWISE) was a spectacular naked object in late 2020 June and early July. The SOHO/SWAN all-sky camera observed its Lyα hydrogen coma on 74 days during the period from 2020 May 13 through September 6. When it was recovered after exiting the SOHO solar avoidance area a few days after perihelion, the hydrogen coma displayed a broad and extended tail produced by solar Lyα radiation pressure that was over 15° long. This was well reproduced by our analysis model that accounts for the nascent velocity distribution and the partial collisional thermalization (and slowing) of atoms as they exit the inner coma. This model was used to calculate water production rates for each image. A maximum water production rate of 5.27 × 10^{30} s^{-1} was recorded on July 8 when the comet was at a heliocentric distance of 0.337 au. While this was one of the largest water production rates ever recorded by SOHO/SWAN (Combi et al. 2019), once the comet was at a heliocentric distance of 1.2–1.3 au, comparable to the perihelion measurements of the Rosetta target comet 67P/Churyumov–Gerasimenko, its production rate was only a factor of ∼3 larger. This, combined with its determined radius

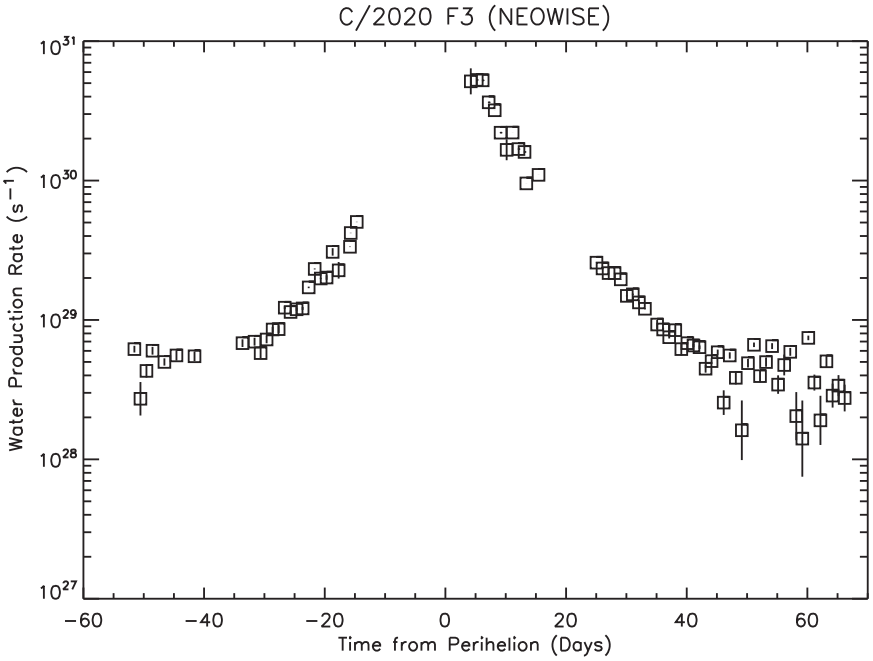

Figure 3. Water production rate in comet C/2020 F3 (NEOWISE) plotted as a function of time in days from perihelion. The error bars indicate the 1 s uncertainties resulting from noise in the data and the fitting of the coma model and interstellar background.

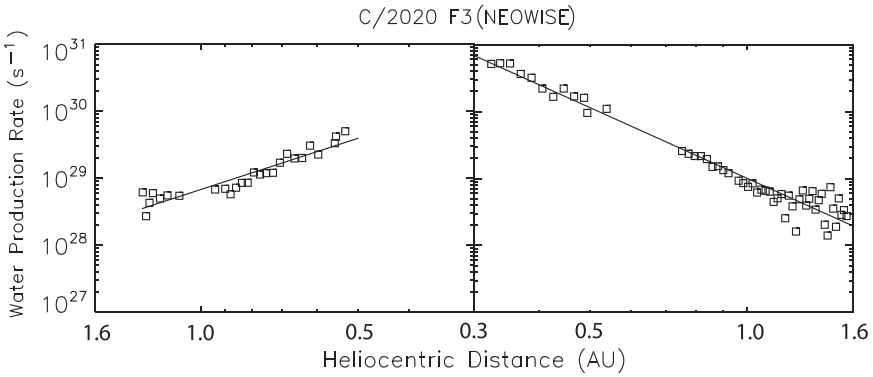

Figure 4. Water production rate of comet C/2020 F3 (NEOWISE) plotted as a function of heliocentric distance. The left half is pre-perihelion and right half is post-perihelion. The straight lines correspond to the power-law fits to the production rate as a function of heliocentric distance for the pre- and post-perihelion legs of the orbit giving values of $(6.9 \pm 0.5) \times 10^{28}\ r^{-2.5\pm0.2}$ and $(10.1 \pm 0.5) \times 10^{28}\ r^{-3.5\pm0.1}$, respectively.

of ∼5 km, compared with that of 67P of ∼4 km, implied that its active fraction was only about a factor of 2 larger than 67P, a rather typical Jupiter-family comet.

The orbit of F3 NEOWISE, having an inbound semimajor axis of 270 au, implies that it is an Old Long-period comet and indicates that it has been through the planetary region of the solar system at least once, and possibly many times. The heliocentric distance dependence, described by power-law fits of production rates as a function of heliocentric distance of $(6.9 \pm 0.5) \times 10^{28}\ r^{-2.5\pm0.2}$ and $(10.1 \pm 0.5) \times 10^{28}\ r^{-3.5\pm0.1}$, respectively, before and after perihelion, are consistent with this dynamical age. There were no noticeable outbursts, quiescent periods, or evidence of any fragmentation throughout the time covered by the SWAN observations.

SOHO is an international mission between ESA and NASA. M. C. acknowledges support from NASA grant 80NSSC18K1005 from the Solar System Observations Program. T.M. was supported by the Finnish Meteorological Institute (FMI). J.-L.B. and E.Q. acknowledge support from CNRS and CNES. We obtained orbital elements from the JPL Horizons website (http://ssd.jpl.nasa.gov/horizons.cgi) and the Minor Planets Center https://www.minorplanetcenter.net. The composite solar Lyα data were taken from the LASP website at the University of Colorado (http://lasp.colorado.edu/lisird/lya/). We acknowledge the personnel that have been keeping SOHO and SWAN operational for over 20 yr, in particular Dr. Walter Schmidt at FMI.

ORCID iDs

M. R. Combi https://orcid.org/0000-0002-9805-0078

References

A'Hearn, M. F., Millis, R. C., Schleicher, D. G., Osip, D. J., & Birch, P. V. 1995, Icar, 118, 223
Bauer, J. M., Mainzer, A., Gicquel, A., et al. 2020, AAS Meeting, 52, 316.04
Bertaux, J. L., Combi, M. R., Quémerais, E., & Schmidt, W. 2014, P&SS, 91, 14

Bertaux, J. L., Costa, J., Quémerais, E., et al. 1998, P&SS, 46, 555
Bertaux, J. L., Kyrölä, E., Quémerais, E., et al. 1995, SoPh, 162, 403
Biver, N., Bockelée-Morvan, D., Hofstadter, D. M., et al. 2019, A&A, 630, A19
Combi, M. 2020a, in urn:nasa:pds:soho:swan_derived::2.0 SOHO SWAN Derived Cometary Water Production Rates Collection, ed. L. Feaga
Combi, M. R., Harris, W. M., & Smyth, W. H. 2004, in Gas Dynamics and Kinetics in the Cometary Coma: Theory and Observations, ed. M. C. Festou, H. U. Keller, & H. A. Weaver (Tucson: Univ. Arizona Press), 523
Combi, M. R., Mäkinen, J. T. T., Bertaux, J.-L., & Quémerais, E. 2005, Icar, 177, 228
Combi, M. R., Mäkinen, T. T., Bertaux, J.-L., Quémerais, E., & Ferron, S. 2019, Icar, 317, 610
Combi, M. R., Reinard, A. A., Bertaux, J.-L., & Quémerais, E. 2000, Icar, 144, 191
Combi, M. R., Shou, Y., Fougere, N., et al. 2020b, Icar, 335, 113421
Combi, M. R., & Smyth, W. H. 1988, ApJ, 327, 1044
Mäkinen, J. T. T., & Combi, M. R. 2005, Icar, 177, 217